ELSEVIER

Nuclear Instruments and Methods in Physics Research A 456 (2001) 342–351

NUCLEAR INSTRUMENTS & METHODS IN PHYSICS RESEARCH Section A

www.elsevier.nl/locate/nima

Single-event upset studies of a high-speed digital optical data link

M.-L. Andrieux[a,*], J. Lundquist[b], B. Dinkespiler[c,1], G. Evans[d], L. Gallin-Martel[a], M. Pearce[b], F. Rethore[c], R. Stroynowski[d], J. Ye[d]

[a]*Institut des Sciences Nucléaires, 53 Avenue des Martyrs, F-38026 Grenoble Cedex, France*
[b]*The Royal Institute of Technology (KTH), Physics Department Frescati, Frescativägen 24, S-10405 Stockholm, Sweden*
[c]*Centre de Physique des Particules de Marseille, 163 Avenue de Luminy, Case 907, F-13288 Marseille Cedex, France*
[d]*Department of Physics, Southern Methodist University, Dallas, TX 75275, USA*

Received 11 February 2000; received in revised form 26 April 2000; accepted 5 June 2000

Abstract

The results from a series of neutron and photon irradiation tests of a high-speed digital optical data link based on a commercial serialiser and a vertical cavity surface emitting laser are described. The link was developed as a candidate for the front-end readout of the ATLAS electromagnetic calorimeter. The components at the emitting end of the link were unaffected by neutron and photon irradiation levels exceeding those expected during 10 years of LHC running. However, the link suffered from Single-Event Upsets (SEUs) when irradiated with energetic neutrons. A very general method based on the Burst Generation Rate (BGR) model has been developed and is used to extrapolate the error rate observed during tests to that expected at the LHC. A model-independent extrapolation was used to check the BGR approach and the results were consistent once systematic errors were taken into account.

PACS: 29.90. + r; 42.81.-i; 42.88. + h; 85.60.-q

Keywords: Radiation tolerance; Single-event upset rate; Gb/s devices; ATLAS

1. Introduction

The Liquid Argon Calorimeter [1] of the ATLAS experiment at the LHC is a highly segmented particle detector with approximately 200 000 channels. Signals generated by particles impacting the calorimeter are small and sensitive to coherent noise. Information derived from these signals is digitised on the detector and subsequently transmitted to data-acquisition electronics situated 100–200 m away. The restricted space available for the signal cables and the need to minimise noise generated by ground loops led to a choice of digital optical links for the data transmission. The front-end electronics has a high degree of multiplexing allowing the calorimeter to be read out over 1600 links each transmitting 32 bits of data at the

* Corresponding author. Tel.: + 33-4-76-28-41-28; fax: + 33-4-76-28-40-04.
E-mail address: m-l.andrieux@isn.in2p3.fr (M-L. Andrieux).
[1] Now at Department of Physics, Southern Methodist University, Dallas, TX 75275, USA.

0168-9002/01/$ - see front matter
PII: S0168-9002(00)00592-1

LHC bunch crossing frequency of 40.08 MHz. A major consideration in the design of the link is the performance in the presence of radiation. The sender part of the link resides in electronics crates which will be exposed to an integrated fluence of 1.7×10^{13} neutrons (1 MeV Si) per cm^2 of the components' surface, an 800 Gy (Si) dose of photons [2] and a three orders of magnitude smaller dose of charged particles over 10 years of LHC running (1 LHC year $= 10^7$ s). These estimates include conservative safety factors.

Early performance tests of the candidate link and irradiation studies are described in Refs. [3,4]. The link is based around Vertical Cavity Surface Emitting Lasers (VCSELs) which were chosen for their radiation tolerance [5]. In this paper, a more detailed study of the link performance in the presence of neutron and photon radiation is described and Single-Event Upset (SEU) characteristics are emphasised. Photon radiation has no effect on the silicon-based electronic components of the present set-up. Its effect on optical fibres is found to depend on fibre composition [6]. During the neutron irradiation studies of the link, transient data transmission errors have been observed and identified as SEUs [7]. The rate of observed SEUs is extrapolated to that expected at the LHC. The extrapolation requires a knowledge of the expected neutron spectrum in ATLAS, which is obtained from detector simulations. It also requires that the dependence of the error rate on the incoming neutron energy is understood. Various neutron sources have been used experimentally: a 2.5 MeV neutron generator with a deuteron beam impinging on a deuteron target and cyclotrons with deuteron (proton) beams with tunable energies ranging from 5 MeV (20 MeV) up to 25 MeV (34 MeV) impinging on a beryllium target. Data has been interpreted using two independent methods: (1) the Burst Generation Rate Model [7] and (2) a model-independent extraction of the error rate using several neutron beams with different energy spectra.

2. Optical link description

A schematic overview of the demonstrator link is shown in Fig. 1. The demonstrator link is based on

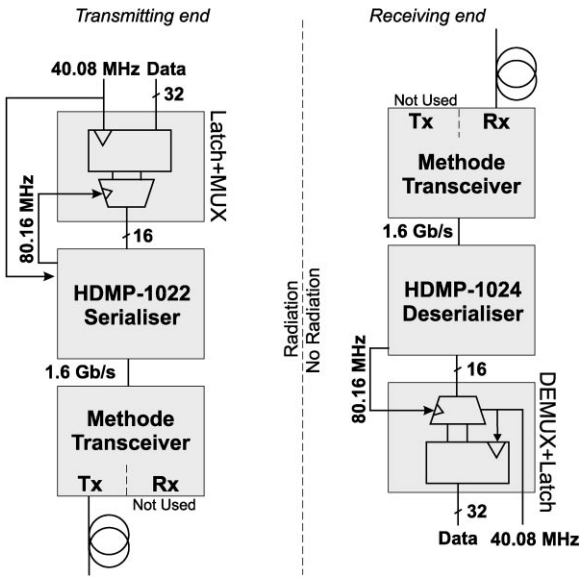

Fig. 1. A Gb/s demonstrator link based on the G-link chipset.

an Agilent Technologies[2] HDMP1022/1024 serialiser/deserialiser set (commonly known as 'G-link') [8], a VCSEL emitting light at a wavelength of 850 nm, a GRaded INdex (GRIN) 50/125 μm optical fibre and a PIN diode. The VCSEL and PIN diode were packaged together with driving and discriminating circuits as transceiver modules.

Data is loaded into the G-link serialiser (Tx) and is delivered to the deserialiser (Rx) over a serial channel. The G-link is operated in double-frame mode: the addition of external (de)multiplexing elements allows a 32 bit data word to be sent as two 16 bit segments. The G-link chip set provides link-down and single-error monitoring through the addition of a 4 bit control field appended to each 16 bit data segment. A 'link-down flag' occurs when the G-link receiver cannot identify a frame to lock onto and a 'single-error flag' indicates an illegal control field in the transmitted frame. The control field denotes the data type being sent and contains a 'master transition' which the receiver uses for frequency locking. The addition of the control field results in a total link data rate of 1.6 Gb/s.

[2] Formally Hewlett Packard.

The monolithic silicon bipolar transmitter and receiver chips are packaged in an aluminium M-Quad 80 package. The G-link transmitter has a PECL serial output and can be connected directly to the input of standard optical transceiver modules. Inside the transceiver modules, the transmitter part consists of a driver circuit coupled to a VCSEL. The receiver contains a PIN photodiode, discriminator and a preamplifier assembly. The transmitter and receiver can be coupled to an optical fibre with an industry standard SC connector.

A Programmable Logic Array (ALTER-AEMP7128) is placed on the receiver board to facilitate demultiplexing and to interface error and link-down flags to the data-acquisition system. The demonstrator link has been tested successfully in the laboratory and no errors were seen during several months of operation. This result exceeds the specified 10^{-14} bit error rate.

3. Radiation facilities and dosimetry

3.1. Neutron irradiations

The neutron irradiations were carried out at three different places:

- SARA (Grenoble, France): a detailed description of this facility can be found in Ref. [9]. The neutron source consists of a thick beryllium target, 35 mm in diameter, bombarded with a 5 μA beam of 20 MeV deuterons. A high neutron flux is obtained via stripping reactions. The neutron energy distributions obtained from $d + Be \rightarrow n$ reactions are illustrated in Fig. 2a (derived from Ref. [10] with a neutron energy detection threshold of 1 MeV). The mean neutron energy measured at SARA is 6 MeV (the neutron energy detection threshold was 100 keV). During irradiation, the link components were mounted on an aluminium plate approximately 30 cm from the target.

  A typical neutron flux experienced by link components was $(2.5 \pm 0.4) \times 10^{11}$ n cm^{-2} h^{-1} or about two orders of magnitude larger than that expected at the LHC. Neutron fluences were measured with an accuracy of $\simeq 1.5\%$ using passive monitors based on an activation method [9] using the charge exchange reaction ^{58}Ni(n,p)^{58}Co. The SARA facility is now closed.
- CERI (Orléans, France): the SARA and CERI neutron production mechanisms and dosimetry are identical but the energy of the incident deuteron (proton) beam is tuneable from 5 MeV (8 MeV) up to 25 MeV (34 MeV) at CERI. Data were taken at the deuteron beam energies of 5, 7, 14, 20 and 25 MeV (20, 25, 30 and 34 MeV). The neutron energy distributions obtained from

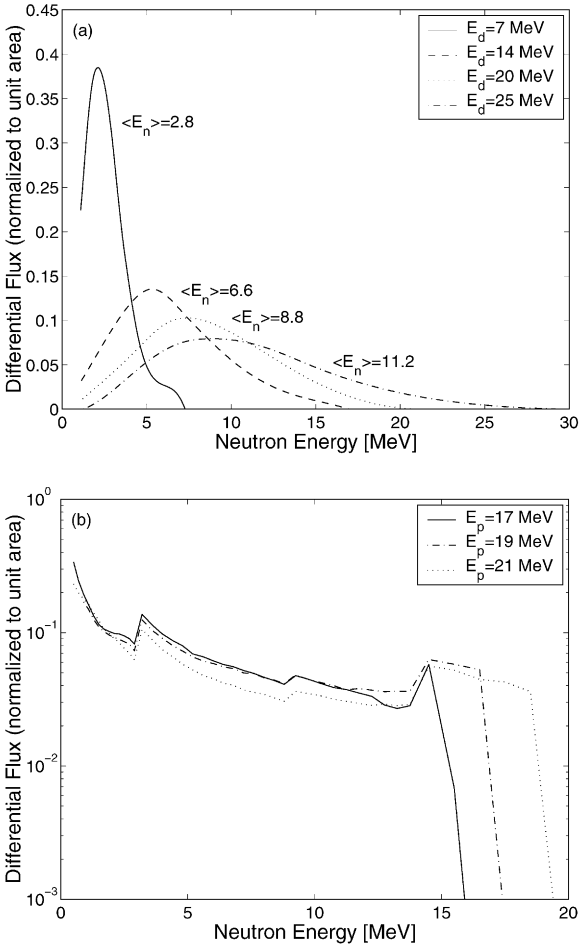

Fig. 2. The neutron energy spectra obtained from (a) $d + Be \rightarrow n$ for various incident deuteron beam energies (this figure is derived from Ref. [10] and the neutron energy detection threshold is 1 MeV) and (b) $p + Be \rightarrow n$ for various incident proton beam energies (this figure is derived from Ref. [11] and the neutron energy detection threshold is 500 keV).

d + Be → n (p + Be → n) reactions are illustrated in Fig. 2a (Fig. 2b – derived from Ref. [11] where a neutron energy detection threshold of 500 keV was applied). The irradiated components were placed 10 cm from the target. The CERI neutron flux was kept constant while the incident beam energies were varied and was identical to that used at SARA: $(2.5 \pm 0.4) \times 10^{11}$ n cm^{-2} h^{-1}. This was achieved by taking the neutron yield (n/nA s sr) distribution as a function of the incident beam energy from Refs. [9,12]. At a fixed incident beam energy the neutron flux is proportional to the incident beam current.

- Chalmers (Göteborg, Sweden): the neutron source comprises of a deuteron beam impinging on a deuteron target producing essentially monoenergetic neutrons of energy 2.5 MeV. The Chalmers neutron flux was 3.6×10^9 n cm^{-2} h^{-1}. The neutron fluences were measured using a calibrated neutron counter placed 1 m from the target.

3.2. Gamma irradiations

The gamma irradiations were performed at Karolinska Hospital [3] in Stockholm using a ^{60}Co source with gamma ray emissions at 1.17 and 1.33 MeV. The delivered dose was approximately 80 Gy h^{-1}. Polymer analine dosimeters were fixed onto the components under test. Doses could be measured with an accuracy of $\simeq 4\%$.

4. Testing procedure and results

4.1. Experimental procedure

Several link sender boards (see Fig. 1) were exposed to both neutron and gamma fluxes to assess the radiation tolerance of the G-link serialiser and different commercial transceivers. No additional link elements, e.g. the multiplexer, were exposed to the radiation. A development in a qualified radiation-tolerant technology is envisaged for the multiplexer.

During irradiation tests, the behaviour of the link was monitored on-line using the G-link's inbuilt error-detection functionality (see Section 2). Two different aspects were investigated: the sender part of the link must withstand a total neutron fluence equivalent to 10 years of LHC running (total dose studies) and the radiation-induced bit error rate in the link must be acceptable (transient error rate studies).

4.2. Results of the neutron-irradiation tests

The neutron total dose studies of the link components demonstrated that the G-link serialiser withstands doses of 5×10^{13} (1 MeV Si) neutrons cm^{-2} which corresponds to about 40 years of LHC running. Among the commercial LAN transceivers tested only those produced by Methode Electronics Inc. tolerated such neutron doses. More details concerning these tests can be found in Refs. [3,4].

The on-line link performance tests showed that transient errors ('single' or 'link-down' error flags) occurred under neutron radiation. For a fixed neutron flux the error rate depended on the average energy ($\langle E_n \rangle$) of the incoming neutron beam (see Fig. 3a). A test carried out at the Chalmers facility showed that 2.5 MeV neutrons induce no errors in the link indicating that the process-generating errors has a threshold at a neutron energy greater than 2.5 MeV.

The error rate dependence with the neutron flux was demonstrated at the SARA facility by varying the intensity of the incident deuteron beam. This result is shown in Fig. 3b.

4.3. Results of the gamma irradiation tests

The radiation tolerance of the sender part of the link has been tested up to a total dose of 800 Gy (Si). Additionally, the G-link chip was exposed up to 3000 Gy (Si), which corresponds to 40 years of LHC running. Unlike the neutron irradiation tests, no transient errors of any kind were observed.

5. Neutron-induced single-event upset analysis

5.1. Error causing processes

There are many possible sources of radiation-induced transient errors in silicon-based electronics.

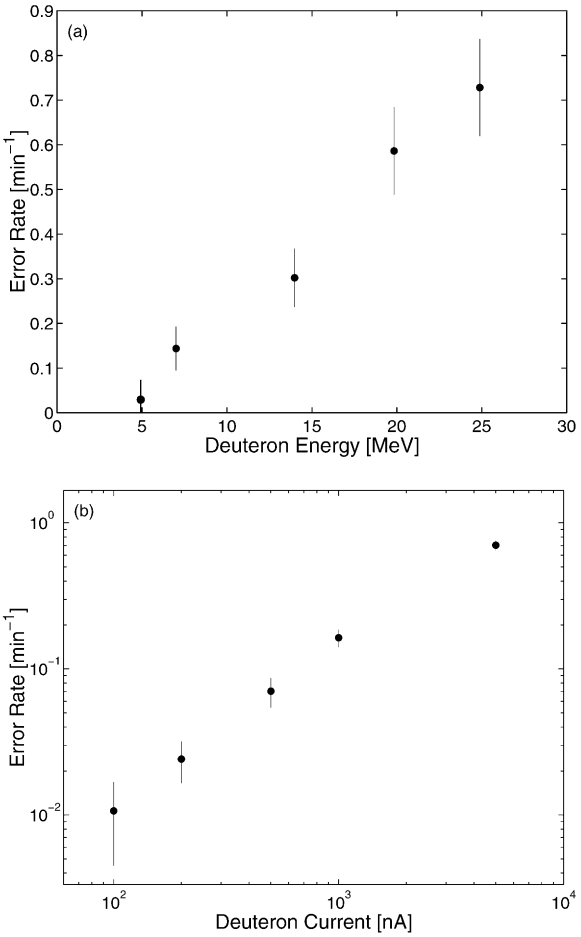

Fig. 3. The transient error rate (a) at a fixed neutron flux ($(2.5 \pm 0.4) \times 10^{11}$ n cm^{-2} h^{-1}) as a function of the incident deuteron beam energy ($\langle E_n \rangle$ scan), and, (b) at a fixed deuteron beam energy (20 MeV) as a function of the incident deuteron beam current (which is proportional to the neutron flux), the 5 μA measurement corresponds to a nominal flux of $(2.5 \pm 0.4) \times 10^{11}$ n cm^{-2} h^{-1}.

The most common ones are due to the passage of ionising particles through the sensitive volume of the device [13–15]. Charged particles can be produced through a number of nuclear reactions induced by neutrons:

- recoil nuclei from elastic neutron scattering:

$$n + Si^{28} \rightarrow n + Si^{28}$$

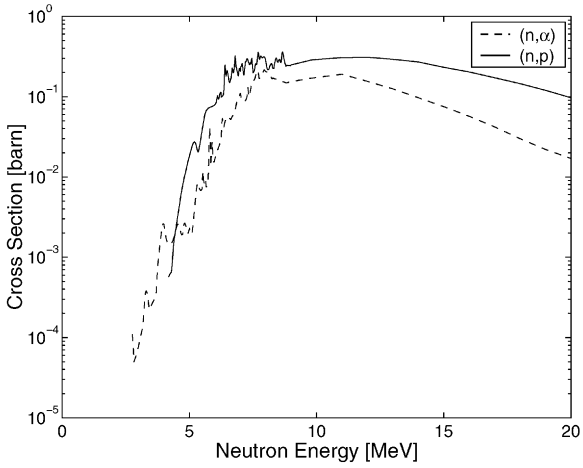

Fig. 4. The cross sections for p and α production in silicon, $n + Si^{28} \rightarrow p + Al^{28}$ and $n + Si^{28} \rightarrow \alpha + Mg^{25}$, as a function of the neutron energy [16].

- inelastic reactions producing protons and alpha particles:

$$n + Si^{28} \rightarrow p + Al^{28}$$

$$n + Si^{28} \rightarrow \alpha + Mg^{25}$$

- nuclear fragmentation:

$$n + Si^{28} \rightarrow n + \alpha + X$$

and others (e.g. inelastic scattering (n, n′), (n, n′p), (n, n′α)).

The interaction of a neutron with silicon produces a shower of secondary particles in the chip and a nuclear recoil or in some cases several fragments. The (n, n), (n,α) and (n, p) reactions are dominant [7] for neutrons with an energy smaller than 20 MeV. For higher-energy neutrons, the main reactions leading to transient errors are the non-elastic reactions with several decay products in the final state. The cross sections for p and α production in silicon as a function of the neutron energy are illustrated in Fig. 4.

The main parameters that need to be taken into account in order to estimate the SEU rate are the sensitive volume of the chip under test and the critical energy which needs to be deposited within the sensitive volume to create upset.

The probability that a charged particle emerging from the collision will traverse a sensitive section of the electronic device depends on the distance from the production point. To produce a SEU typically requires energy deposition exceeding a few hundred keV. Due to kinematic considerations, no SEU is expected for neutrons with an energy below $\simeq 2.5$ MeV (see Section 4.2 and Refs. [14,15]), except for a possible effect due to the interaction of thermal neutrons with boron (^{10}B(n,α)^{7}Li) dopants in the chip. However, the conclusions of recent studies published in Refs. [14,15] state that thermal neutrons do not play an important role in SEU at the LHC when compared with the effects induced by higher-energy neutrons.

5.2. Burst generation rate model

Neutrons interacting with silicon produce ionising recoils from nuclear reactions of the type (n, n), (n, p) and (n, α). These reactions and the energy deposition they induce can be analysed in terms of the 'Burst Generation Rate' (BGR) model [13]. This model has been defined in terms of a partial macroscopic cross section (BGR (E_n, E_r)) for neutrons of energy E_n to produce recoils of energy E_r or greater. This cross section can be applied to the differential neutron energy spectrum (dN/dE_n) to estimate the SEU rate. The BGR method of calculating the rate of neutron-induced SEUs due to recoils has been shown to be effective [16] in other applications.

The definition given in Ref. [7] has been used in the present analysis:

$$\frac{d\,SEU}{dt} = VCg\int_{E_n} BGR(E_n, E_r)(dN/dE_n)\,dE. \qquad (1)$$

Here, V is the sensitive volume of the chip (μm^3), C is the collection efficiency (fraction of charge released by the recoil collected in V) and g is an additional correction factor (e.g., to account for contributions from light ions). Note that the product VCg depends strongly on the intrinsic parameters of the device under test. Consequently, it can be extracted as a constant factor from the experimental data.

5.3. Application to the CERI experimental data

The BGR model applied to the CERI like neutron spectra (d + Be → n and p + Be → n) implies that the integral:

$$I_{BGR} = \int_{E_n} BGR(E_n, E_r)(dN/dE_n)\,dE$$

is proportional to the measured error rate at CERI.

In the present analysis, the BGR(E_n, E_r) functions illustrated in Fig. 5 are taken from Ref. [17]. To perform the I_{BGR} calculation they are combined with the differential neutron energy spectra taken from Refs. [10,11,18]. The neutron spectrum produced by p + Be → n interactions with $E_p = 34$ MeV is measured at the CERI facility [19]. In the I_{BGR} calculation the neutron spectra detailed above are normalised to unit area.

The χ^2 dependence of the recoil energy E_r in a linear fit of the measured SEU rate (d + Be → n and p + Be → n CERI experimental data) versus I_{BGR} is shown in Fig. 6. The optimal value of E_r (denoted E_{opt}) where the χ^2 minimises is $E_{opt} = 0.5 \pm 0.4$ MeV.

In Fig. 7, the SEU upset rates recorded during CERI experiments are compared with the results of previous BGR calculations for $E_r = E_{opt}$. The two sets of CERI measurements (and the respective

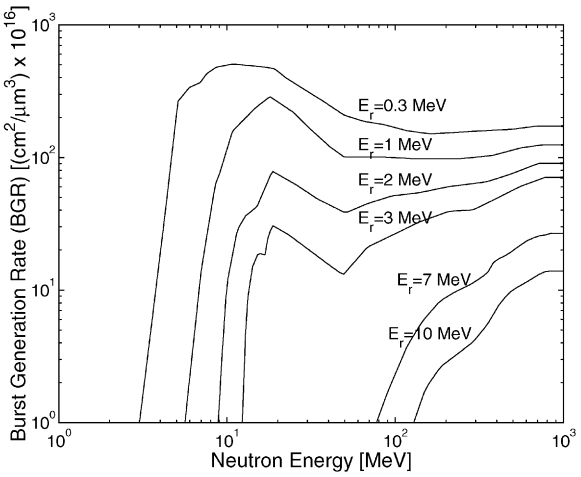

Fig. 5. BGR (E_n, E_r) functions for neutrons of energy E_n creating recoils of energy E_r or greater [16].

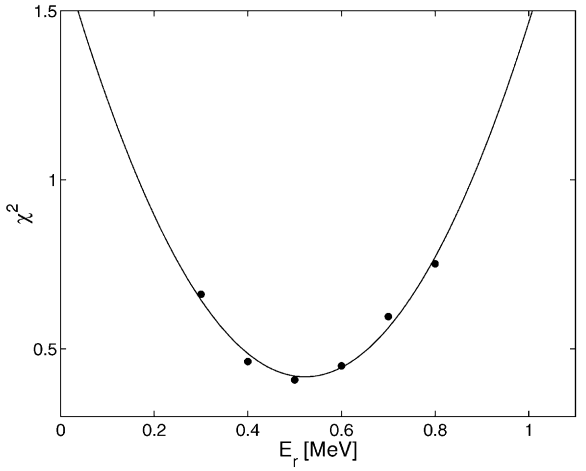

Fig. 6. Results from a χ^2 analysis to determine the optimal value of E_r from a linear fit of the CERI SEU rate measurements (d + Be → n and p + Be → n) versus I_{BGR}.

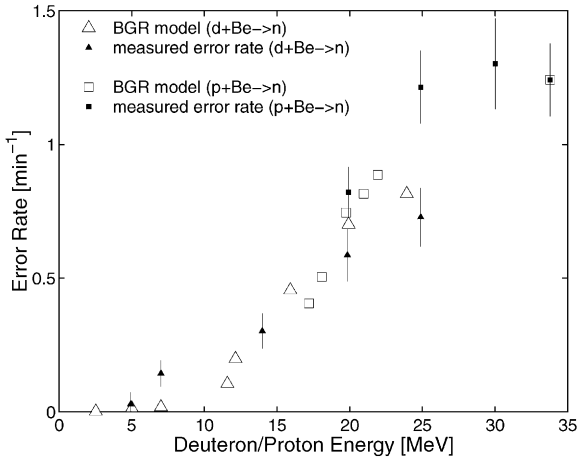

Fig. 7. Two sets of CERI measurements (d + Be → n and p + Be → n) plotted together with the respective BGR model calculations for the optimal value of the BGR recoil energy parameter ($E_r = E_{opt}$).

BGR model calculations) are plotted together: d + Be → n with E_d ranging from 5 MeV (2.6 MeV) up to 25 MeV (24 MeV) and p + Be → n with E_p ranging from 20 MeV (17 MeV) up to 34 MeV (34 MeV).

The model and the experimental results are in close agreement.

6. Single-event upset rate estimate in ATLAS

6.1. ATLAS-like conditions

The aim of this study is to extrapolate the SEU rate measured at the neutron irradiation facilities to that expected in ATLAS during the running of the experiment. The differences between the expected neutron fluxes and energy spectra must be accounted for.

There are independent calculations of the expected neutron flux in ATLAS [2,20,21]. The predictions of the total neutron flux agree and differences in the detailed spectral shapes can be ascribed mainly to the differences in the modelling of the detector. The estimated total neutron flux at ATLAS is two orders of magnitude lower than at CERI [20,21].

The neutron energy spectrum calculated for the location of calorimeter electronics crates is shown in Fig. 8 together with a representative experimental neutron test spectrum. In this study, the portion of the neutron spectrum below 2.5 MeV has been neglected since an apparent threshold for the SEUs (see Section 4.2) has been observed. For a 20 MeV deuteron beam at CERI approximately 85% of the neutron energy spectrum is above 2.5 MeV. In ATLAS this percentage is significantly lower: 14 ± 9% [20,21].

6.2. Application of the BGR method

In Eq. (1) the CERI-like neutron spectra are replaced by that expected in ATLAS [20]. The product VCg has been deduced from analysis of CERI data for each E_r value in the range $E_{opt} = 0.5 \pm 0.4$ MeV.

Using the BGR method the ATLAS error rate is estimated at 0.005 ± 0.003 error/link/h. This results only takes into account the G-link in-built error flags. A refined CERI test where the content of data words was checked led to an estimate of 0.013 ± 0.006 error/link/h. This value is multiplied by a safety factor of 5 to take into account the uncertainties in the simulation of the ATLAS neutron spectrum [2]. Consequently, the expected error rate may be as high as 0.065 ± 0.030 error/link/h.

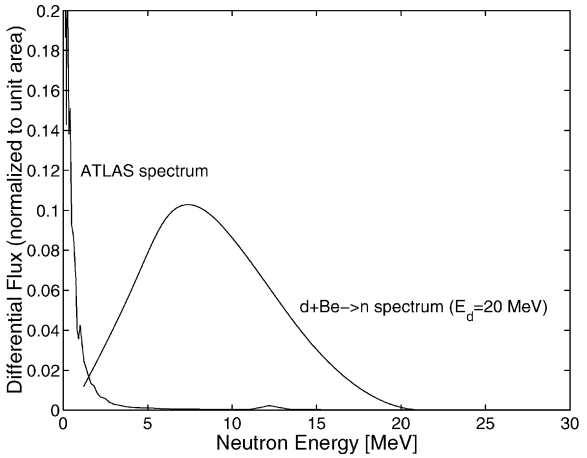

Fig. 8. A comparison of the ATLAS neutron energy spectrum with the experimental spectrum corresponding to $d + Be \rightarrow n$ and $E_d = 20$ MeV. The curves are normalised. The ATLAS neutron spectrum peaks strongly at low energies and so the y-axis is truncated at 0.2.

6.3. Model-independent extraction of the error rate

The BGR model depends on a large number of assumptions about the processes contributing to the SEU rate and about the composition of the chip under test. During the irradiation tests, SEU rates were measured using neutrons generated by deuterons and protons beams at several different energies but with an identical neutron flux. For each incident beam energy the neutron energy spectrum spanned different, and often overlapping, ranges. This allows the probability for a neutron of a given energy to generate SEU to be derived directly from data. For each CERI incident beam energy (E_{beam}), the measured error rate, N_i(error), is given by an integral of the product of the probability for a neutron at a given energy to produce an error over the neutron energy spectrum:

$$\int_{E_n} P(E_n) \times (dN/dE_n)_i \, dE = N_i(\text{error}). \quad (2)$$

Here, P is the probability for a neutron of energy E_n to create an error and $(dN/dE_n)_i$ is the differential neutron flux (n/cm^2 s MeV) associated to each E_{beam} value. In the present analysis only seven CERI measurements out of nine were used ($i = 1, \ldots, 7$). The p + Be $\rightarrow$ n SEU measurements with $E_p = 25$ and 30 MeV were excluded since no differential neutron flux data was available. As in the BGR model analysis, the neutron spectra used in this analysis were normalised to unit area and taken from Refs. [10,11,18,19] ($E_p = 34$ MeV).

The neutron energy range spanned by the seven CERI measurements can be divided into seven bins in order to extract the values of P_j, defined as the probability for a neutron in the $(\Delta E_n)_j$ energy range to create SEU:

$$\begin{aligned}
P_1&: && && E_n \leq 3.5 \text{ MeV}\\
P_2&: && 3.5 \text{ MeV} && < E_n \leq 7.0 \text{ MeV}\\
P_3&: && 7.0 \text{ MeV} && < E_n \leq 10.0 \text{ MeV}\\
P_4&: && 10.0 \text{ MeV} && < E_n \leq 14.0 \text{ MeV}\\
P_5&: && 14.0 \text{ MeV} && < E_n \leq 20.0 \text{ MeV}\\
P_6&: && 20.0 \text{ MeV} && < E_n \leq 26.0 \text{ MeV}\\
P_7&: && 26.0 \text{ MeV} && < E_n.
\end{aligned}$$

Eq. (2) can be rewritten as a sum over each $(\Delta E_n)_j$ energy range defined above:

$$\sum_j P_j \int_{(\Delta E_n)_j} (dN/dE_n)_i \, dE = N_i(\text{error}) \quad (3)$$

and recast as a matrix product

$$M \times P = N \quad (4)$$

where M is the square matrix (7×7) associated with the coefficients $m_{i,j}$:

$$m_{i,j} = \int_{(\Delta E_n)_j} (dN/dE_n)_i \, dE$$

and P and N are the vectors associated to P_j and N_i(error), respectively.

From Eq. (4) the P_j values (j ranges from 1 to 7) can be deduced.

Using a procedure similar to that described for the BGR method (see Section 6.1), the ATLAS neutron energy spectrum is used in Eq. (3) where i now equals to 1 and an ATLAS-like error rate is extracted: 0.018 error/link/h. As for the BGR calculations, this value should be multiplied by a safety factor of 5 to account for uncertainties on the ATLAS neutron energy spectrum. Consequently,

the expected error rate may be as high as 0.090 errors/link/h. This is compatible with the BGR model expectations which can be as high as 0.065 ± 0.030 error/link/h.

6.4. Discussion

The results obtained from the two methods described in the previous sections are consistent. The BGR method leads to a possible SEU rate in ATLAS of 0.065 ± 0.030 error/link/h (including a conservative safety factor of 5). The technique to measure and then to extrapolate to ATLAS-like conditions is general and does not depend on the detailed composition of the electronics component under test.

In the G-link-based set-up, a large fraction (about 50%) of the SEUs results in a loss of synchronisation between the serialiser and deserialiser chips (a 'link-down error'). The re-synchronisation of the chip set can take up to few milliseconds. All information transmitted during this time is lost. An ATLAS SEU rate of 0.065 ± 0.030 error/link/h implies a dead time of the order of 10^{-5} for the entire calorimeter (1600 links). To reduce this number, a possible solution for ATLAS is a dual G-link system carrying identical information on two independent links and a fast switch on the receiving end selecting the uncorrupted data. In such a design, the probability for two links to be down due to SEU at the same time is negligible.

7. Conclusions

A 1.6 Gb/s demonstrator link based on the commercial G-link chipset has been built and tested in a neutron and gamma radiation environment. The components have been found to be radiation tolerant at least up to 1.7×10^{13} n (1 MeV Si) cm^{-2} and 800 Gy gamma radiation which corresponds to 10 years of LHC running including safety factors [2]. No adverse effects have been observed during gamma irradiations up to 3000 Gy using a ^{60}Co source. The radiation tolerance of a G-link serialiser coupled to a Methode transceiver has also been demonstrated under neutron radiation up to 5×10^{13} (1 MeV Si) neutrons/cm^2.

Transient errors were observed during neutron irradiations, but none were seen during gamma irradiations. Two different approaches have been used to estimate the single event upset rate in ATLAS-like conditions. The first is based on the Burst Generation Rate (BGR) model and leads to a possible ATLAS error rate of 0.065 ± 0.030 error/link/h (including a safety factor of 5 to account for uncertainties in the ATLAS neutron spectrum [2]). A simple matrix inversion method based on experimental data confirms the BGR method estimate of ATLAS single-event upset rate. The BGR model method is general and could be used to study the single event upset rate for any type of electronic set-up.

Acknowledgements

Financial support from Institut National de Physique Nucléaire et de Physique des Particules (IN2P3), Forskningsrådsnämnden (FRN), Naturvetenskapliga Forskningsrådet (NFR) and US Department of Energy, is acknowledged. Paola Sala and Michael Shupe from the ATLAS Collaboration are thanked for fruitful discussions and for the ATLAS radiation levels and neutron energy spectra maps. The operations and technical crews at each of the irradiation facilities (CERI, Chalmers, Karolinska Hospital, SARA) are thanked for their help.

References

[1] The ATLAS Collaboration, Liquid Argon Calorimeter Technical Design Report, CERN/LHCC/96-41, December 1996.

[2] Ph. Farthouat et al., ATLAS Policy on Radiation Tolerant Electronics, ATLAS Internal Note ELEC-NO-003, 1997.

[3] M.L. Andrieux et al., Development of radiation tolerant Gb/s optical links for the front-end read-out of the ATLAS Liquid Argon Calorimeter, Proceedings of the Fourth Workshop on Electronics for LHC Experiments, Rome, Italy, September 21–25, 1998.

[4] M.L. Andrieux et al., Nucl. Phys. B (Proc. Suppl.) 78 (1999) 719.

[5] M.-L. Andrieux et al., Nucl. Instr. and Meth. A 426 (1999) 332.

[6] G. Mahout et al., ATLAS note ATL-ELEC-99-001, Nucl. Instr. and Meth. A 446 (2000), 426.
[7] E. Normand, W. Ross Doherty, IEEE, Trans. Nucl. Sci. 36 (1989) 2349.
[8] Hewlett Packard – Agilent devices more details can be found at http://www.semiconductor.agilent.com/fiber/gigabit_home.html.
[9] J. Collot et al., Nucl. Instr. and Meth. A 350 (1994) 525.
[10] C.J. Parnell, British J. Radiol. 45 (1972) 452.
[11] H.J. Brede et al., Nucl. Instr. and Meth. A 274 (1989) 332.
[12] S.W. Johnsen, Medical Phys. 4 (3) (1977) 255.
[13] J.F. Ziegler, W.A. Landford, Science 206 (1979) 776.
[14] M. Huhtinen, F. Faccio, Nucl. Instr. and Meth. A 450 (2000), 155.
[15] F. Faccio, C. Detcheverry, M. Huhtinen, Proceedings of the Fourth Workshop on Electronics for LHC Experiments, Rome, Italy, September 21–25, 1998.
[16] ENDF/B-VI database, more details can be found at http://is.nea.fr/html/dbdata/nds_evaluated.htm.
[17] E. Normand et al., IEEE, Trans. Nucl. Sci. 45 (1998) 2904.
[18] J.W. Meadows, Nucl. Instr. and Meth. A 324 (1993) 239.
[19] The CERI Facility Management, private communications.
[20] P. Sala, ATLAS collaboration, private communications.
[21] M. Shupe, ATLAS collaboration, private communications.